Polymer Chemistry

Cite this: *Polym. Chem.*, 2012, **3**, 2949

www.rsc.org/polymers

PAPER

Synthesis and photovoltaic properties of new conjugated polymers based on *syn*- and *anti*-benzodifuran†

Chao Hu,[a] Yingying Fu,[b] Shugang Li,[a] Zhiyuan Xie*[b] and Qing Zhang*[a]

Received 8th July 2012, Accepted 6th August 2012
DOI: 10.1039/c2py20504a

Donor–acceptor conjugated polymers based on benzo[1,2-*b*:5,4-*b*′]difuran (*syn*-BDF) or benzo [1,2-*b*:5,4-*b*′]difuran (*anti*-BDF) as donors and isoindigo as acceptors were synthesized by Stille cross-coupling reaction. The effects of *syn*- and *anti*-repeating units on optical, electrochemical and photovoltaic properties of polymers were investigated. The ***anti*-PBDFID** displayed lower optical bandgap and higher HOMO energy level than ***syn*-PBDFID**. The ***syn*-PBDFID** had better solubility than ***anti*-PBDFID**. The energy levels of two new polymers were compared with some related benzo [1,2-*b*:4,5-*b*′]dithiophenes (BDTs) based polymers. The results suggested that the utilization of less conjugated repeating units such as *syn*-BDF and the elimination of electron donating groups on the central phenyl ring of BDF can effectively lower the HOMO energy level of polymer. The low HOMO energy level of ***syn*-PBDFID** enabled high open circuit voltages in PSC devices.

Introduction

Research on conjugated polymers for organic photovoltaic (OPV) applications has attracted much attention. Polymer solar cells (PSCs) are considered to be a promising alternative for producing clean energy at low cost. Many new conjugated polymers have been synthesized and achieved high power conversion efficiencies (PCEs) in PSC devices.[1–11] Design of new monomers may open up new possibilities for novel polymers with tailored optical and electrochemical properties.[12–18] Recently, benzo[1,2-*b*:4,5-*b*′]dithiophenes (BDTs) with rigid planar π-conjugated structures and tunable redox properties have been successfully incorporated into many high performance polymers for OPV applications.[19–21] Furan contains only the first row elements. Oligofurans have shown tighter packing and smaller reorganization energy than their thiophene counterparts.[22] Furan based materials also show significantly improved solubilities.[23,24] Furans have become attractive building blocks for the synthesis of conjugated polymers. The furanyl counterparts of BDTs have also been synthesized. The polymers based on alkoxy substituted benzo[1,2-*b*:4,5-*b*′]difurans (BDFs) showed smaller optical bandgap than the related polymers based on BDTs. The BDF based polymers also displayed comparable PSC device performances as the related polymers based on BDTs.[25,26]

Due to the electron-rich character of furan, oligo- and polyfurans are more electron-rich than their thienyl counterparts.[22–24] The polymers containing furanyl moieties frequently show higher HOMO energy levels than similar polymers containing thienyl moieties.[22,25] The PCE is the product of the short-circuit current density (J_{sc}), open circuit voltage (V_{oc}) and fill factor (FF) divided by the incoming light power density. It is known that the V_{oc} of bulk-heterojunction (BHJ) solar cell devices with PCBM as acceptor is determined by the HOMO level of the donor and the LUMO level of the acceptor molecule.[27] The high-lying HOMO of the polymer can limit the maximum open-circuit voltage and may cause oxidative instability of solar cell device at ambient conditions. In a donor–acceptor alternating polymer, the HOMO energy level is mainly determined by the electron-donor and the LUMO energy level is mainly related to the electron-acceptor.[28] The design and synthesis of less electron-rich furan containing monomers are necessary to reduce the HOMO energy level of polymers and therefore for achieve high V_{oc} in OPV devices. The benzodifuran have both *syn*- and *anti*-isomers. So far, only the alkoxy substituted *anti*-isomers have been studied as building blocks for synthesis of conjugated polymers.[25,26] *Syn*-isomers have never been used as repeating units in polymer. Herein, we reported the synthesis of both benzo[1,2-*b*:5,4-*b*′]difuran (*syn*-BDF) and benzo[1,2-*b*:4,5-*b*′] difuran (*anti*-BDF) monomers. Both new monomers were designed without electron donating alkoxy groups on the central phenyl rings for increasing ionization potentials. Two new conjugated polymer ***syn*-PBDFID** and ***anti*-PBDFID** based on isoindigo as acceptors and *syn*- or *anti*-BDF as donors were synthesized. The optical, electrochemical and photovoltaic properties of polymers were investigated. The ***syn*-PBDFID** displayed lower HOMO

[a]*Department of Polymer Science and Engineering, School of Chemistry and Chemical Engineering, Shanghai Jiao Tong University, Shanghai 200240, P. R. China. E-mail: qz14@sjtu.edu.cn*
[b]*State Key Laboratory of Polymer Physics and Chemistry, Changchun Institute of Applied Chemistry, Chinese Academy of Science, Changchun 130022, China. E-mail: xiezy_n@ciac.jl.cn*

† Electronic supplementary information (ESI) available: NMR spectra for monomers and copolymers, TGA analysis for copolymers. See DOI: 10.1039/c2py20504a

energy level than ***anti*-PBDFID**. The ***syn*-PBDFID** also achieved higher V_{oc} than ***anti*-PBDFID** in solar cell devices.

Results and discussion

1. Synthesis and characterization

The synthetic routes for monomers and polymers are shown in Scheme 1. The *syn*-BDF[29] and *anti*-BDF were synthesized from dehydrogenation of 2,3,5,6-tetrahydrobenzo[1,2-*b*:5,4-*b*′]difuran and 2,3,6,7-tetrahydrobenzo[1,2-*b*:4,5-*b*′]difuran, respectively. The 2,3-dichloro-5,6-dicyano-1,4-benzoquinone (DDQ) was used as oxidation reagent. The bis(trimethylstannyl) monomer **1** and **3** were obtained through lithiation of corresponding BDFs and followed by quenching with trimethyltin chloride in 82% and 85% yield, respectively. The synthesis of isoindigo monomer was reported in our previous work.[30] Isoindigo is an electron-deficient building block for conjugated polymers.[31] The polymer ***syn*-PBDFID** and ***anti*-PBDFID** were synthesized by Stille cross-coupling reaction in the presence of tris(dibenzylidene-acetone) dipalladium as catalyst and tri-*o*-tolylphosphine as ligand. The polymers were purified by washing sequentially with methanol and hexane in a Soxhlet extractor for 24 h each, and then were extracted with hot chloroform in a Soxhlet extractor for 12 h. After removing solvent under reduced pressure, dark blue solids were collected. Polymer ***syn*-PBDFID** showed better solubility than polymer ***anti*-PBDFID**. ***syn*-PBDFID** was completely soluble in chloroform and chlorobenzene. A part of ***anti*-PBDFID** was not soluble in hot chloroform or chlorobenzene and cannot be extracted in hot chloroform solution. This resulted in low yield of ***anti*-PBDFID**. The low solubility of ***anti*-PBDFID** can be attributed to the strong interchain aggregation which was caused by linear structured repeating units.[32]

2. Thermal stability

Thermogravimetric analyses of ***syn*-PBDFID** and ***anti*-PBDFID** are shown in Fig. S9 (see ESI†). Both polymers showed good thermal stabilities with decomposition temperatures over 400 °C. Furan oligomers such as hexamer usually displayed relatively low decomposition temperatures (~250 °C).[22] The high decomposition temperatures of ***syn*-PBDFID** and ***anti*-PBDFID** indicated that fused aromatic structures did increase the thermal stabilities of materials. Neither polymers showed noticeable glass transition in differential scanning calorimetry (DSC) analysis (Fig. S10†).

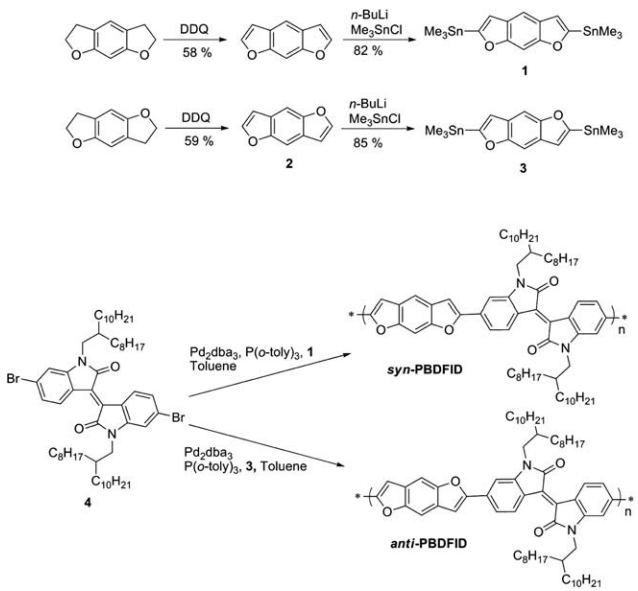

Scheme 1 Synthesis of monomers and polymers.

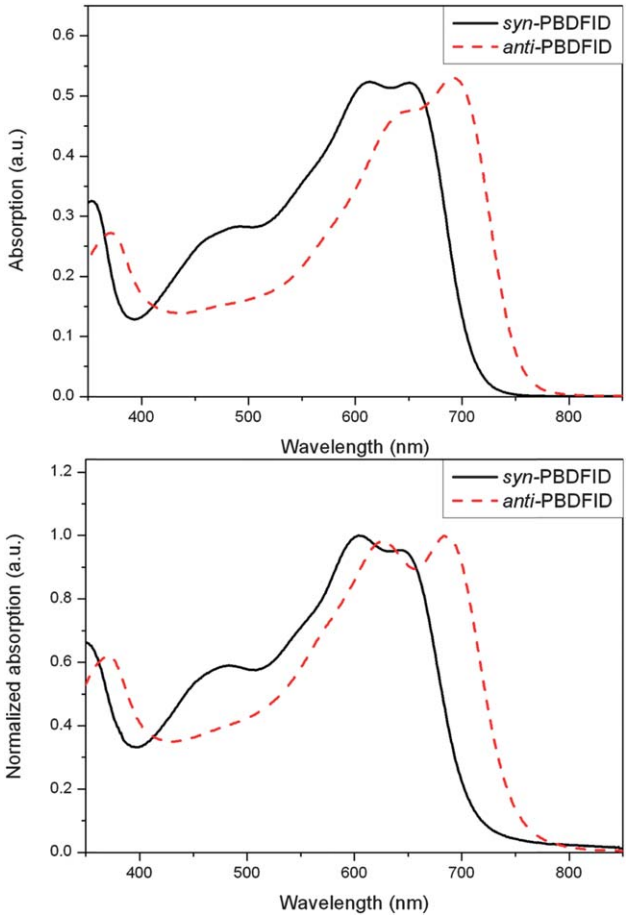

Fig. 1 UV-vis absorption spectra of ***syn*-PBDFID** and ***anti*-PBDFID** in chloroform solution (1.0×10^{-5} M) and as thin films.

3. Optical properties

The UV-vis absorption spectra of ***syn*-PBDFID** and ***anti*-PBDFID** in dilute chloroform solution are shown Fig. 1 (top) and the spectra of thin films are shown in Fig. 1 (bottom). The optical properties of polymers are summarized in Table 1. The maximum absorptions were at 651 nm and 692 nm for ***syn*-PBDFID** and ***anti*-PBDFID** in dilute chloroform solution, respectively; and the maximum absorptions were at 604 nm and 684 nm for ***syn*-PBDFID** and ***anti*-PBDFID** as thin film, respectively. The spectra of ***anti*-PBDFID** were red-shifted compared with the spectra of ***syn*-PBDFID**. The absorption maxima of polymer thin-films were slightly blue-shifted compared with the absorption maxima of the polymers in dilute chloroform solution for both polymers. Similar phenomenon were observed for other isoindigo-containing conjugated polymers.[33] The onset absorption edges of the

Table 1 Optical and electrochemical properties of polymers

	UV-vis absorption						
Copolymers	λ_{max}[a]	λ_{max}[b]	λ_{onset} (in film)	E_g^{opt}[c] (eV)	E_{ox}^{onset} (V)	HOMO[d] (eV)	LUMO (eV)[e]
***syn*-PBDFID**	616, 651	604, 644	715	1.73	0.92	5.63	3.90
***anti*-PBDFID**	634, 692	626, 684	754	1.64	0.78	5.49	3.85

[a] In chloroform solution (1.0×10^{-5} M). [b] As thin-film. [c] $E_g^{opt} = 1240/\lambda_{onset}$ (in film). [d] HOMO $= -e(E_{ox}^{onset} + 4.71\ V)$. [e] LUMO $= E_g^{opt} + E_{ox}^{onset}$.

thin-films were at 715 nm and 754 nm for ***syn*-PBDFID** and ***anti*-PBDFID**, respectively. Accordingly, the optical bandgaps were calculated to be 1.73 eV and 1.64 eV for ***syn*-PBDFID** and ***anti*-PBDFID**, respectively (Table 1). The onset absorption edges of ***anti*-PBDFID** thin film showed a red-shift of 39 nm compared with that of ***syn*-PBDFID** thin-film. This red-shift indicated that ***anti*-PBDFID** had a better conjugation in polymer backbone than ***syn*-PBDFID**. The extended conjugation resulted in small bandgap through the reducing of the LUMO energy and raising of the HOMO energy.[15]

4. Electrochemical properties

The cyclic voltammograms of the polymers are displayed in Fig. S11,† and the electrochemical properties are summarized in Table 1. Both ***syn*-PBDFID** and ***anti*-PBDFID** showed semi-reversible oxidation cycles but no reduction cycle. The HOMO energy levels were calculated from the onset oxidations with reference to Fc/Fc^+ at −4.8 V.[34] The HOMO energy levels of ***syn*-PBDFID** and ***anti*-PBDFID** were −5.63 eV and −5.49 eV, respectively (Table 1). The LUMO energy levels of ***syn*-PBDFID** and ***anti*-PBDFID** were at −3.90 eV and −3.85 eV, which were calculated from the optical band gap and HOMO energy levels of the polymers, respectively. The energy levels of new polymers were compared with some related isoindigo based polymers with different **BDT** units (Fig. 2). The ***syn*-PBDFID** showed lower HOMO level than ***anti*-PBDFID**. The ***anti*-PBDFID** showed slightly lower HOMO energy than thienyl substituted polymer **PBDTTID**. Both ***syn*-PBDFID** and ***anti*-PBDFID** showed significantly lower HOMO energy than alkoxy substituted polymer **PBDTID**.[30] The utilization of a less conjugated structure such as *syn*-BDF and elimination of electron donating groups on the central phenyl ring resulted in the low HOMO energy of ***syn*-PBDFID**.

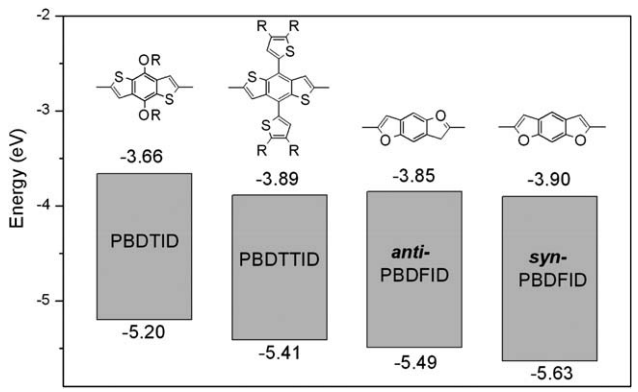

Fig. 2 Energy levels of isoindigo based polymers with different donors.

5. Photovoltaic properties

Bulk hetero-junction (BHJ) PSC devices with polymer ***syn*-PBDFID** and ***anti*-PBDFID** as electron donors and $PC_{71}BM$ as electron acceptor were fabricated. The device structure was ITO/PEDOT:PSS/polymer:$PC_{71}BM$/LiF/Al. The weight ratio of polymer to $PC_{71}BM$ in active layer was 1 : 2. The devices were optimized with different processing solvents (Table 2). Chlorobenzene was found to be the best solvent for processing both ***syn*-PBDFID** and ***anti*-PBDFID**. The optimized device based on ***syn*-PBDFID** had a thickness of 60 nm. The illuminated current–voltage curves of the devices based on ***syn*-PBDFID**/$PC_{71}BM$ are displayed in Fig. 3. The device gave a short circuit current (J_{sc}) of 2.89 mA cm^{-2}, a fill factor (FF) of 0.59, an open-circuit voltage (V_{oc}) of 0.85 V and resulted in a PCE of 1.44%. The illuminated current–voltage curves for the devices based on ***anti*-PBDFID**/$PC_{71}BM$ are displayed in Fig. 4. The optimized device based on ***anti*-PBDFID**/$PC_{71}BM$ had a thickness of 65 nm. The device gave a J_{sc} value of 1.74 mA cm^{-2}, a FF value of 0.48, a V_{oc} value of 0.75 V and resulted in a PCE of 0.65%. The effect of processing additive on the device performance was also investigated. The results are listed in Table 2. For ***syn*-PBDFID**, the addition of 1,8-diiodoctane (DIO, 1.0% by volume) increased the J_{sc} of corresponding devices slightly (from 2.89 mA cm^{-2} to 3.02 mA cm^{-2}), decreased the FF (from 0.59 to 0.51), maintained the V_{oc} value of 0.85 V and resulted in a slightly lower PCE 1.32% (Fig. 3). For ***anti*-PBDFID**, the addition of DIO (1.0% by volume) increased the J_{sc} of corresponding devices from 1.74 mA cm^{-2} to 2.80 mA cm^{-2}, decreased the FF from 0.48 to 0.38, decreased the V_{oc} value from 0.75 V to 0.61 V and resulted in a PCE value of 0.65% (Fig. 4). The non-ideal characteristic *J-V* curves might be attributed to non-optimized morphology or interface barriers. The external quantum efficiency (EQE) curves for the devices based on ***syn*-PBDFID** and ***anti*-PBDFID** processed with additive are displayed in Fig. 5. The ***syn*-PBDFID** based device showed higher EQE values than the ***anti*-PBDFID** based device in the region of 350 to 615 nm. This may result from more efficient light absorption of ***syn*-PBDFID** in the region and better morphology of ***syn*-PBDFID**/$PC_{71}BM$ active layer. The ***anti*-PBDFID** based devices achieved better EQE values than the ***syn*-PBDFID** based device in the region of 615 to 750 nm. This resulted from more efficient light absorption of ***anti*-PBDFID** based active layer in the region.

6. Morphology

The morphology plays an important role in the device performances. Proper morphology is necessary not only for exciton dissociation but also for charge transport to respective

Table 2 Solar cell characteristic of polymers: $PC_{71}BM$ blends (1 : 2, w/w)

	Device					
Copolymers	Solvent	Active layer thickness (nm)	V_{oc} (V)	J_{sc} (mA cm^{-2})	FF	PCE (%)
***syn*-PBDFID**	CF	85	0.80	1.28	0.50	0.53%
	CB	60	0.85	2.89	0.59	1.44%
	o-DCB	55	0.79	2.83	0.48	1.07%
	CB, with 1 vol% DIO	60	0.85	3.02	0.51	1.32%
***anti*-PBDFID**	CF	80	0.67	1.19	0.48	0.38%
	CB	65	0.75	1.74	0.48	0.65%
	o-DCB	50	0.53	2.36	0.39	0.48%
	CB, with 1 vol% DIO	65	0.61	2.80	0.38	0.65%

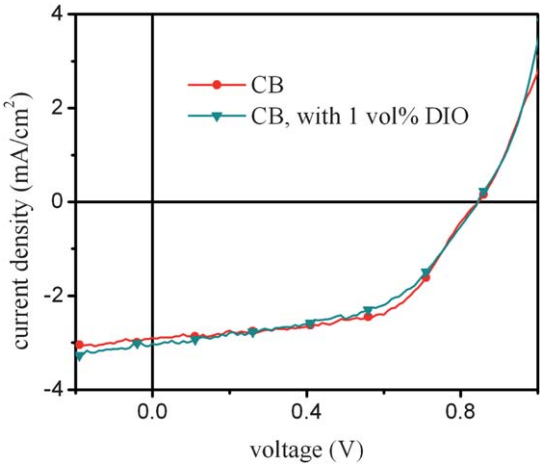

Fig. 3 Illuminated *J*–*V* curves of PSC devices based on ***syn*-PBDFID**/$PC_{71}BM$ (1 : 2, w/w) fabricated from CB with or without DIO (1% by volume).

contacts.[35] Atomic force microscopy (AFM) was used to investigate the morphology of polymer/$PC_{71}BM$ active layer. Topography and phase images were taken from the film of polymer/$PC_{71}BM$ blends cast from chlorobenzene (CB) with or without DIO as processing additive (Fig. 6). Both ***syn*-** and ***anti*-PBDFID**/$PC_{71}BM$ blends processed from CB without DIO displayed large phase separations, which led to poor exciton dissociation efficiency and finally low J_{sc}. Many different solution systems were used for fabricating the active layer of ***anti*-PBDFID**/$PC_{71}BM$. However, appropriate morphology was never achieved. If the morphology had improved, the J_{sc} would have been increased. Moreover, the ***anti*-PBDFID**/$PC_{71}BM$ blend showed higher surface roughness and much larger average domain size than ***syn*-PBDFID**/$PC_{71}BM$ blend. These results suggested that the low performances of ***anti*-PBDFID** based devices were likely due to the poor morphology of ***anti*-PBDFID**/$PC_{71}BM$ blends. The ***anti*-PBDFID** had much lower solubility than the ***syn*-PBDFID**. The precondition for achieving optimized morphology is the good miscibility of two materials. The inherent low solubility of ***anti*-PBDFID** may result in incompatibility between polymer and the $PC_{71}BM$ acceptor. The addition of DIO (1% by volume) reduced the domain size and slightly improved surface roughness for both polymer blends. As a result, the J_{sc} of devices fabricated with DIO as processing additives were slightly increased due to the more efficient charge generation.

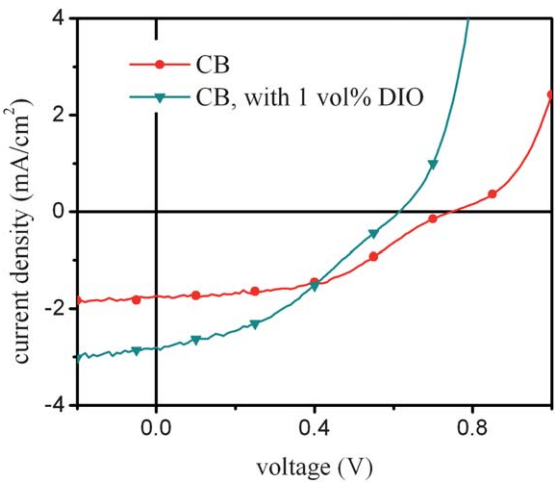

Fig. 4 Illuminated *J*–*V* curves of PSC devices based on ***anti*-PBDFID**/$PC_{71}BM$ (1 : 2, w/w) fabricated from CB with or without DIO (1% by volume).

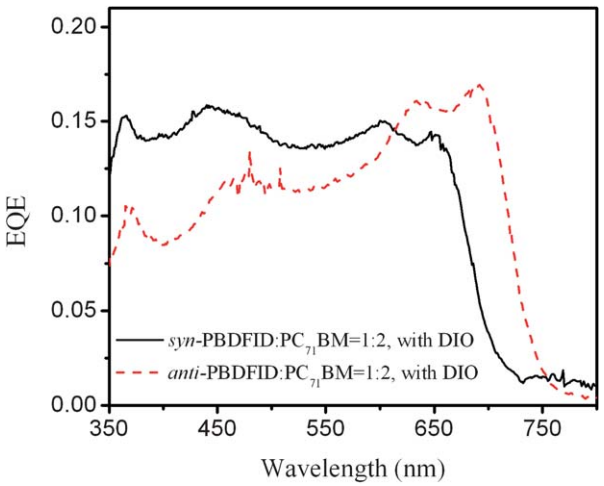

Fig. 5 EQE spectra of PSC devices based on ***syn*-PBDFID**/$PC_{71}BM$ (1 : 2, w/w) and ***anti*-PBDFID**/$PC_{71}BM$ (1 : 2, w/w) fabricated from chlorobenzene with DIO added (1% by volume).

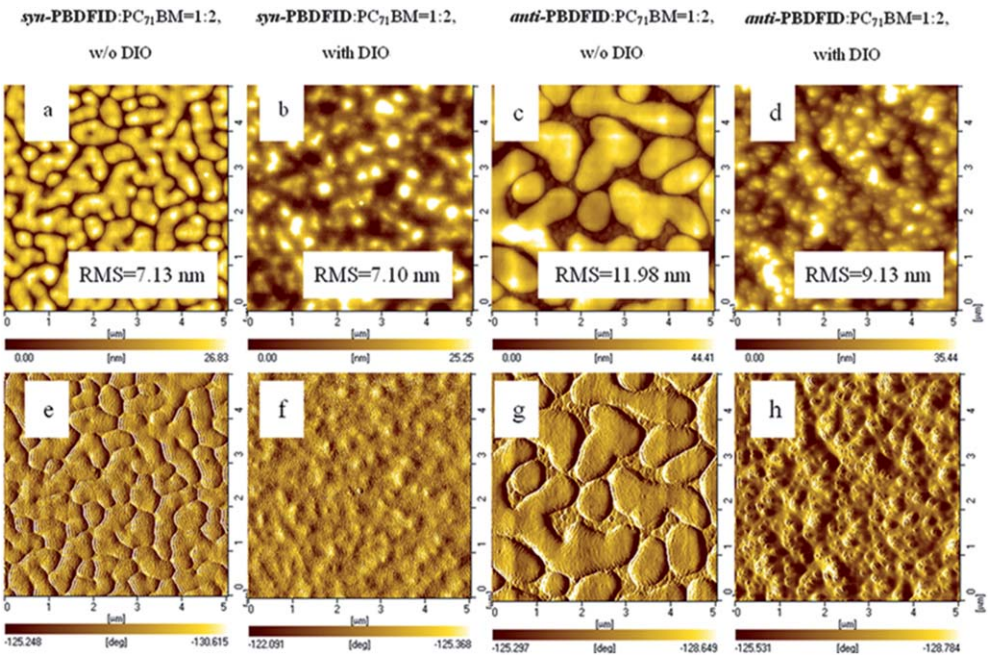

Fig. 6 AFM images of active layers processed from chlorobenzene, topography images (a–d) and phase images (e–h).

Experimental

1. Instrumentation

Nuclear Magnetic Resonance (NMR) spectra were recorded on a Mercury plus 400 MHz machine. Elemental analyses were performed on an Elementar vario EL III elemental analysis instrument. Gel permeation chromatography (GPC) measurements were performed on a Shimadzu LC-20A GPC coupled with differential refractive index detector using tetrahydrofuran as eluent with polystyrenes as standards. Thermogravimetric analyses (TGA) were conducted with a TA instrument Q5000IR at a heating rate of 20 °C min^{-1} under nitrogen gas flow. Differential scanning calorimetry (DSC) analysis was performed on a Perkin Elmer instrument Pyris 1 in nitrogen atmosphere. All the samples (about 10.0 mg in weight) were first heated up to 300 °C and held for 2 min to remove thermal history, followed by the cooling at rate of 20 °C min^{-1} to 20 °C and then heating at rate of 20 °C min^{-1} to 300 °C. UV-vis absorption spectra were recorded on a Perkin Elmer model lambda 20 UV-vis spectrophotometer. Electrochemical measurements were conducted on a CS-150 electrochemical analyzer under nitrogen in a deoxygenated anhydrous acetonitrile solution of tetra-*n*-butylammonium hexafluorophosphate (0.1 M). A platinum disc electrode was used as a working electrode, a platinum-wire was used as an auxiliary electrode, and an Ag/Ag^{+} electrode was used as a reference electrode. Thin film of polymer was coated on the surface of platinum disc electrode and ferrocene was chosen as a reference.

2. Device fabrication and characterization

Polymer solar cells (PSCs) with the device structures of ITO/PEDOT:PSS/polymer:$PC_{71}BM$ (1 : 2, w/w)/LiF/Al were fabricated as follows: a *ca.* 40 nm thick PEDOT:PSS (Baytron P AI 4083) was spin-coated from an aqueous solution onto the pre-cleaned ITO substrates and was dried at 120 °C for 30 min in air. Then the substrates were transferred into a nitrogen filled glove box. The mixture of polymer and $PC_{71}BM$ in a chosen solvent with or without DIO was spin-coated on top of the PEDOT/PSS layer. The samples were transferred into an evaporator. LiF (1 nm) and Al (100 nm) layers were thermally deposited under a vacuum of 10^{-6} Torr with area of 0.12 cm^2. The devices were encapsulated in the glove box and measured in the air. Current–voltage characteristics were measured using a computer controlled Keithley 236 source meter. The photocurrents were measured under AM 1.5G illumination at 100 mW cm^{-2} from a solar simulator (Oriel, 91160A-1000). The EQEs were measured at a chopping frequency of 280 Hz with a lock-in amplifier (Stanford, SR830) during illumination with the monochromatic light from a xenon lamp. The AFM measurements were performed on SPA300HV instrument with an SPI3800 controller (Seiko Instruments).

3. Materials

Chemicals were purchased from Sigma-Aldrich Chemical Company, Alfa Aesar Chemical Company, Sinopharm Chemical Reagent Co. Ltd. and Darui Chemical Co. Ltd. Tetrahydrofuran and toluene were freshly distilled over sodium wire under nitrogen prior to use. Other materials were used without further purification.

4. Synthesis of monomers and polymers

2,6-Bis(trimethyltin)-benzo[1,2-*b*:5,4-*b*′]difuran (1). A solution of *n*-butyllithium (2.9 mL, 7.0 mmol, 2.4 M in hexane) was added dropwise to *syn*-BDF[29] (0.50 g, 3.16 mmol) in tetrahydrofuran (40 mL) at −78 °C. The mixture was stirred at −78 °C for 30 min, and then was stirred at 0 °C for 1 h. Trimethyltin chloride (7.0 mL, 7.0 mmol, 1.0 M in hexane) was added slowly to the

mixture. After stirred at −78 °C for 1.5 h, it was warmed to room temperature and was stirred for 2 h. The reaction was quenched with addition of water (100 mL) and the mixture was extracted with diethyl ether (60 mL) for three times. The combined organic layer was dried with anhydrous sodium sulfate. Solvent was removed under reduced pressure and the residue was purified by recrystallization in *iso*-propanol to afford a white solid (1.25 g, 82%). ^{1}H NMR (400 MHz, $CDCl_3$), δ(ppm): 7.61 (s, 1H), 7.59 (s, 1H), 6.96 (s, 2H), 0.42 (s, 18H). ^{13}C NMR (100 MHz, $CDCl_3$), δ(ppm): 165.37, 157.26, 124.82, 117.82, 109.45, 93.64, −8.92. Anal. Calcd for $C_{16}H_{22}O_2Sn_2$: C, 39.72; H, 4.58%. Found: C, 39.46; H, 4.62%.

Benzo[1,2-*b*:4,5-*b*′]difuran (2). A degassed solution of 2,3-dichloro-5,6-dicyano-1,4-benzoquinone (DDQ) (10.16 g, 44.76 mmol) in dry 1,4-dioxane (100 mL) was add slowly to a degassed solution of 2,3,6,7-tetrahydrobenzo[1,2-*b*:4,5-*b*′]difuran[36] (2.20 g, 13.56 mmol) in dry 1,4-dioxane (150 mL). The mixture was refluxed for 24 h under nitrogen. After cooled to room temperature, the mixture was passed through a short pad of silica gel. The filtrate was collected, the solvent was removed under reduced pressure and residue was purified by chromatography on silica gel, eluting with petroleum ether (boiling range 60–90 °C) to give the product as a white solid (1.26 g, 59%).^{1}H NMR (400 MHz, $CDCl_3$), δ(ppm): 7.67 (s, 2H), 7.66 (d, J = 2.4, 2H), 6.84 (d, J = 2.4, 2H). ^{13}C NMR (100 MHz, $CDCl_3$), δ(ppm): 152.25, 145.92, 125.71, 107.00, 102.35.

2,6-Bis(trimethyltin)-benzo[1,2-b:4,5-b′]difuran (3). A solution of *n*-butyllithium (2.9 mL, 7.0 mmol, 2.4 M in hexane) was added dropwise to **2** (*anti*-BDF) (0.50 g, 3.16 mmol) in tetrahydrofuran (40 mL) at −78 °C. The mixture was stirred at −78 °C for 15 min, and then stirred at 0 °C for 30 min. Trimethyltin chloride (7.0 mL, 7.0 mmol, 1.0 M in hexane) was added slowly to the mixture. After stirred at −78 °C for 30 min, it was warmed to room temperature and was stirred for 1 h. The reaction was quenched with addition of water (100 mL) and the mixture was extracted with diethyl ether (60 mL) for three times. The combined organic layer was dried with anhydrous sodium sulfate. Solvent was removed under reduced pressure and the residue was purified by recrystallization in *iso*-propanol to afford a white solid (1.30 g, 85%). ^{1}H NMR (400 MHz, $CDCl_3$), δ(ppm): 7.59 (s, 2H), 6.99 (s, 2H), 0.44 (s, 18H). ^{13}C NMR (100 MHz, $CDCl_3$), δ(ppm): 166.26, 155.80, 126.00, 118.09, 100.65, −8.88. Anal. Calcd for $C_{16}H_{22}O_2Sn_2$: C, 39.72; H, 4.58%. Found: C, 39.69; H, 4.65%.

Synthesis of polymer *syn*-PBDFID. Tris(dibenzylideneacetone) dipalladium (0.009 g, 0.010 mmol) and tri-*o*-tolylphosphine (0.012 g, 0.040 mmol) were added to a solution of compound **1** (0.242 g, 0.500 mmol) and compound **4** (0.520 g, 0.530 mmol) in toluene (20.0 mL) under nitrogen. The solution was subjected to three cycles of evacuation and admission of nitrogen. The mixture was heated to 110 °C for 8 h. After cooled to room temperature, the mixture was poured into methanol (100 mL) and was stirred for 2 h. The precipitate was collected by filtration. The product was purified by washing with methanol and hexane in a Soxhlet extractor for 24 h each. It was extracted with hot chloroform in a Soxhlet extractor for 24 h. After removing the solvent, a dark blue solid was collected (0.36 g, 74%). ^{1}H NMR ($CDCl_3$, 400 MHz), δ(ppm): 9.0–9.1 (br, 2H), 6.2–7.5 (br, 8H), 3.4–4.1 (br, 4H), 0.3–2.5 (br, 78H). GPC: M_n = 146.8 kDa; PDI = 2.34.

Synthesis of polymer *anti*-PBDFID. Tris(dibenzylideneacetone)dipalladium (0.009 g, 0.010 mmol), tri-*o*-tolylphosphine (0.012 g, 0.040 mmol) were added to a solution of compound **3** (0.242 g, 0.500 mmol) and compound **4** (0.520 g, 0.530 mmol) in toluene (20.0 mL) under nitrogen. The solution was subjected to three cycles of evacuation and admission of nitrogen. The mixture was heated to 110 °C for 8 h. After cooling to room temperature, the mixture was poured into methanol (100 mL) and stirred for 2 h. The precipitate was collected by filtration. The product was purified by washing with methanol and hexane in a Soxhlet extractor for 24 h each. It was extracted with hot chloroform in a Soxhlet extractor for 24 h. After removing solvent, a dark blue solid was collected (0.14 g, 28%). ^{1}H NMR ($CDCl_3$, 400 MHz), δ(ppm): 8.5–9.1 (br, 2H), 6.2–7.6 (br, 8H), 3.5–4.1 (br, 4H), 0.2–2.5 (br, 78H). GPC: M_n = 34.8 kDa; PDI = 2.55.

Conclusions

In summary, new donor–acceptor conjugated polymers based on isoindigo as acceptors and *syn*- or *anti*-BDF as donors were synthesized. The *syn*- and *anti*-BDF based polymers showed different optical, electrochemical and photovoltaic properties. The ***anti*-PBDFID** displayed lower optical bandgap and higher HOMO energy level than ***syn*-PBDFID**. The ***syn*-PBDFID** had better solubility than ***anti*-PBDFID**. The low solubility of ***anti*-PBDFID** may cause incompatibility between polymer and $PC_{71}BM$, and thus result in large-scale phase separation. This is a plausible explanation for low device performances of ***anti*-PBDFID** based solar cells. The energy levels of two new polymers were compared with some related benzo[1,2-*b*:4,5-*b*′]dithiophenes (BDTs) based polymers. The results suggest that the utilization of less conjugated repeating units such as *syn*-BDF and the elimination of electron donating groups on the central phenyl ring of BDF can realize polymer with low HOMO energy level. The low HOMO energy level of ***syn*-PBDFID** enabled high open circuit voltages in PSC devices. We may conclude that these results will provide useful information for the rational design and synthesis of polymers for PSC applications in the future.

Acknowledgements

This work was supported by National Natural Science Foundation of China (NSFC Grant nos. 21174084 and 20834005).

Notes and references

1 H. Y. Chen, J. H. Hou, S. Zhang, Y. Liang, G. Yang, Y. Yang, L. P. Yu, Y. Wu and G. Li, *Nat. Photonics*, 2009, **3**, 649.
2 L. Huo, J. H. Hou, S. Zhang, H. Y. Chen and Y. Yang, *Angew. Chem., Int. Ed.*, 2010, **122**, 1500.
3 C. Dennler, M. C. Scharber and C. Brabec, *Adv. Mater.*, 2009, **21**, 1323.
4 G. Zhao, Y. He and Y. Li, *Adv. Mater.*, 2010, **22**, 4355.
5 J. M. Szarko, J. Guo, Y. Liang, B. Lee, B. S. Rolczynski, J. Strzalka, T. Xu, S. Loser, T. J. Marks, L. P. Yu and L. X. Chen, *Adv. Mater.*, 2010, **22**, 5468.

6 H. J. Son, W. Wang, T. Xu, Y. Y. Liang, Y. Wu, G. Li and L. P. Yu, *J. Am. Chem. Soc.*, 2011, **133**, 1885.
7 H. Zhou, L. Yang, A. C. Stuart, S. C. Price, S. Liu and W. You, *Angew. Chem., Int. Ed.*, 2011, **50**, 2995.
8 T. Y. Chu, J. Lu, S. Beaupre, Y. Zhang, J. R. Pouliot, S. Wakim, J. Zhou, M. Leclerc, Z. Li, J. Ding and Y. Tao, *J. Am. Chem. Soc.*, 2011, **133**, 4250.
9 J. Li, K.-H. Ong, S.-L. Lim, G.-M. Ng, H.-S. Tan and Z.-K. Chen, *Chem. Commun.*, 2011, **47**, 9480.
10 E. G. Wang, Z. Ma, Z. Zhang, K. Vandewal, P. Henriksson, O. Inganäs, F. Zhang and M. R. Andersson, *J. Am. Chem. Soc.*, 2011, **133**, 14244.
11 C. M. Amb, S. Chen, K. R. Graham, J. Subbiah, C. E. Small, F. So and J. R. Reynolds, *J. Am. Chem. Soc.*, 2011, **133**, 10062.
12 G. Yu, J. Gao, J. C. Hummelen, F. A. Wudl and A. J. Heeger, *Science*, 1995, **270**, 1789.
13 J. Peet, J. Y. Kim, N. E. Coates, W. L. Ma, D. Moses, A. J. Heeger and G. C. Bazan, *Nat. Mater.*, 2007, **6**, 497.
14 C. H. Cui, H. J. Fan, X. Guo, M. J. Zhang, Y. J. He, X. W. Zhan and Y. F. Li, *Polym. Chem.*, 2012, **3**, 99.
15 I. McCulloch, R. S. Ashraf, L. Biniek, H. Bronstein, C. Combe, J. E. Donaghey, D. I. James, C. B. Nielsen, B. C. Schroeder and W. M. Zhang, *Acc. Chem. Res.*, 2012, **45**, 714.
16 B. C. Thompson and J. M. J. Fréchet, *Angew. Chem., Int. Ed.*, 2008, **47**, 58.
17 J. W. Chen and Y. Cao, *Acc. Chem. Res.*, 2009, **42**, 1709.
18 S. H. Park, A. Roy, S. Beaupre, S. Cho, N. Coates, J. S. Moon, D. Moses, M. Leclerc, K. Lee and A. J. Heeger, *Nat. Photonics*, 2009, **3**, 297.
19 J. H. Hou, M. Park, S. Zhang, Y. Yao, L. Chen, J. Li and Y. Yang, *Macromolecules*, 2008, **41**, 6012.
20 G. B. Zhang, Y. Y. Fu, Q. Zhang and Z. Y. Xie, *Chem. Commun.*, 2010, **46**, 4997.
21 L. J. Huo and J. H. Hou, *Polym. Chem.*, 2011, **2**, 2453.
22 U. H. F. Bunz, *Angew. Chem., Int. Ed.*, 2010, **49**, 5037.
23 C. H. Woo, P. M. Beaujuge, T. W. Holcombe, O. P. Lee and J. M. J. Fréchet, *J. Am. Chem. Soc.*, 2010, **132**, 15547.
24 (*a*) J. C. Bijleveld, B. P. Karsten, S. G. Mathijssen, J. M. M. Wienk, D. M. Leeuw and R. A. J. Janssen, *J. Mater. Chem.*, 2011, **21**, 1600; (*b*) O. Gidron, Y. Diskin-Posner and M. Bendikov, *J. Am. Chem. Soc.*, 2010, **132**, 2148.
25 L. J. Huo, Y. Huang, B. H. Fan, X. Guo, Y. Jing, M. J. Zhang, Y. F. Li and J. H. Hou, *Chem. Commun.*, 2012, **48**, 3318.
26 Y. P. Zou, X. W. Chen, B. Liu, L. Xiao, X. P. Guo, Y. H. He and Y. F. Li, *J. Mater. Chem.*, 2012, **22**, 17724.
27 M. C. Scharber, D. Mühlbacher, M. Koppe, P. Denk, C. Waldauf, A. J. Heeger and C. J. Brabec, *Adv. Mater.*, 2006, **18**, 789.
28 N. Blouin, A. Michaud, D. Gendron, S. Wakim, E. Blair, R. Neagu-Plesu, M. Belletéte, G. Durocher, Y. Tao and M. Leclerc, *J. Am. Chem. Soc.*, 2008, **130**, 732.
29 J. C. González-Gómez, L. Santana and E. Uriarte, *Tetrahedron*, 2005, **61**, 4805.
30 G. B. Zhang, Y. Y. Fu, Q. Zhang and Z. Y. Xie, *Macromolecules*, 2011, **44**, 1414.
31 (*a*) J. Mei, K. R. Graham, R. Stalder and J. R. Reynolds, *Org. Lett.*, 2010, **12**, 660; (*b*) B. Liu, Y. P. Zou, B. Peng, B. Zhao, K. L. Huang, Y. H. He and C. Y. Pan, *Polym. Chem.*, 2011, **2**, 1156; (*c*) R. Stalder, C. Grand, J. Subbiah, F. Sob and J. R. Reynolds, *Polym. Chem.*, 2012, **3**, 89; (*d*) Z. Ma, E. Wang, M. E. Jarvid, P. Henriksson, O. Inganäs, F. L. Zhang and M. R. Andersson, *J. Mater. Chem.*, 2012, **22**, 2306.
32 R. Rieger, D. Beckmann, A. Mavrinskiy, M. Kastler and K. Müllen, *Chem. Mater.*, 2010, **22**, 5314.
33 Z. F. Ma, E. G. Wang, M. E. Jarvid, P. Henriksson, O. Inganäs, F. L. Zhang and M. R. Andersson, *J. Mater. Chem.*, 2012, **22**, 2306; R. Stalder, J. G. Mei and J. R. Reynolds, *Macromolecules*, 2010, **43**, 8348.
34 J. Pommerehne, H. Vestweber, W. Guss, R. F. Mahrt, H. Bässler, M. Porsch and J. Daub, *Adv. Mater.*, 1995, **7**, 551.
35 P. A. Troshin, H. Hoppe, A. S. Peregudov, M. Egginger, S. Shokhovets, G. Gobsch, N. S. Sariciftci and V. F. Razumov, *ChemSusChem*, 2011, **4**, 119.
36 A. P. Monte, D. Marona-Lewicka, M. A. Parker, D. B. Wainscott, D. L. Nelson and D. E. Nichols, *J. Med. Chem.*, 1996, **39**, 2953.